

2

FILE CARD REPORT DOCUMENT

AD-A210 196

1a. REPORT SECURITY CLASSIFICATION (U) ELECTED

2a. SECURITY CLASSIFICATION AUTHORITY NA JUL 14 1989

2b. DECLASSIFICATION/DOWNGRADING SCHEDULE NA

3. DISTRIBUTION/AVAILABILITY STATEMENT
Distribution Unlimited

4. PERFORMING ORGANIZATION REPORT NUMBER(S)
Massachusetts Institute of Technology.

5. MONITORING ORGANIZATION REPORT NUMBER(S)
NA

6a. NAME OF PERFORMING ORGANIZATION
Massachusetts Institute of Technology.

6b. OFFICE SYMBOL (if applicable)
NA

7a. NAME OF MONITORING ORGANIZATION
Office of Naval Research

6c. ADDRESS (City, State, and ZIP Code)
Harvard-MIT Div. of Health, Sciences and Technology, Mass. Institute of Technology, 77 Mass. Avenue, Cambridge, Mass. 02139.

7b. ADDRESS (City, State, and ZIP Code)
800 North Quincy Street
Arlington, VA. 22217-5000.

8a. NAME OF FUNDING/SPONSORING ORGANIZATION
Office of Naval Research

8b. OFFICE SYMBOL (if applicable)
ONR

9. PROCUREMENT INSTRUMENT IDENTIFICATION NUMBER
N00014-87-K-0479.

8c. ADDRESS (City, State, and ZIP Code)
800 North Quincy Street
Arlington, VA. 22217-5000

10 SOURCE OF FUNDING NUMBERS			
PROGRAM ELEMENT NO.	PROJECT NO.	TASK NO.	WORK UNIT ACCESSION NO
61153N	RR04108	441K709.	

11. TITLE (Include Security Classification)
(U) Electroporation: Theory of Basic Mechanisms.

12. PERSONAL AUTHOR(S)
James C. Weaver, Principal Investigator

13a. TYPE OF REPORT
Annual Project

13b. TIME COVERED
FROM 06/01/88 TO 05/31/89

14. DATE OF REPORT (Year, Month, Day)
89/6/30

15. PAGE COUNT
51

16. SUPPLEMENTARY NOTATION

17. COSATI CODES		
FIELD	GROUP	SUB-GROUP

18. SUBJECT TERMS (Continue on reverse if necessary and identify by block number)
electroporation, bilayer membranes, cell membranes, membrane channels, bioelectrochemistry.

19. ABSTRACT (Continue on reverse if necessary and identify by block number)
Electroporation is a dramatic and apparently universal phenomenon which occurs in all bilayer-containing membranes. For this reason electroporation has implications for basic understanding of cell membranes, and is also likely to lead to a number of new applications. A quantitative understanding of how electroporation occurs has been lacking. We report significant progress towards providing descriptions of mechanisms which can quantitatively account for most of the complex electrical behavior of planar bilayer membranes without proteins. This has set the stage for development of models which describe both electrical behavior and molecular transport.

20. DISTRIBUTION/AVAILABILITY OF ABSTRACT
 UNCLASSIFIED/UNLIMITED SAME AS RPT. DTIC USERS

21. ABSTRACT SECURITY CLASSIFICATION
U

22a. NAME OF RESPONSIBLE INDIVIDUAL
Dr. James C. Weaver

22b. TELEPHONE (Include Area Code)
(617)253-4194.

22c. OFFICE SYMBOL

R & T Code
Date: 30 June 1989

PROGRESS REPORT ON CONTRACT N00014-87-K-0479

CONTRACTOR: Massachusetts Institute of Technology

PRINCIPAL INVESTIGATOR: James C. Weaver

CONTRACT TITLE: Electroporation: Theory of Basic Mechanisms

INTRODUCTION

The objective of our investigation is the development of a theory of the mechanism of electroporation. Overall we seek to find models which allow theoretical description of measurable quantities. This includes the more specific objective of first providing a quantitative description of key features of electrical behavior, and subsequently of molecular transport.

In summary form, electroporation (i) is now believed to be a universal cell membrane phenomenon, involving both the lipid bilayer and membrane macromolecules, and is therefore fundamental to membrane understanding, (ii) provides a general method for introducing molecules into cells, or releasing molecules from cells, with potentially major applications in science and technology, and yet (iii) its mechanism is poorly understood.¹⁻³ For example, no previous theory actually describes electrical behavior during electroporation, membrane recovery, or the amount of molecular transport.

APPROACH TO A THEORETICAL MODEL

Keywords: Membrane, Electroporation, Bioelectrochemistry, etc.

With this in mind, our specific goals have been:

- (1) Extension of an initial theory of reversible electrical breakdown to one with more solid foundations, i.e. elimination of the approximate "switch on" criteria of pores, and elimination of the assumption of the membrane containing so many pores that the membrane was "saturated" with pores.⁴ A significant advance towards this goal has been made, and is presented in a recently submitted paper (copy appended).
- (2) Achievement of a theory which quantitatively describes the transmembrane potential, $U(t)$, during irreversible rupture, such that a unified theory of both REB and rupture is provided by one model. Such a theory should yield predictions of $U(t)$ which can be compared directly with experiments, a basic requirement of which has not yet been achieved by other theories of electroporation. This has recently been accomplished, and is presented in the appended manuscript.
- (3) Related achievement of the ability to quantitatively describe incomplete REB, i.e. a discharge that stops before the transmembrane potential reaches zero. This has also been achieved (see appended manuscript).

89 7 13 039

- (4) Extension of our first, successful theory of the reversible electrical breakdown of electroporation to include metastable pores associated with a "foot-in-the-door" mechanism, i.e. a molecule/pore interaction wherein the presence of a macromolecule partially inserted within a pore prevents the pore from shrinking and then vanishing. This approach, based on the approximation of one-dimensional diffusion through the long lifetime pore, is a candidate mechanism for molecular transport associated with electroporation.
- (5) Further extension to include a pore-membrane macromolecule interaction in the theory. Membrane channel proteins are prime candidates for such interactions, and may provide nucleation sites for the long lifetime pores which are believed to occur. Such metastable pores may have significantly longer lifetimes than "ordinary" transient aqueous pores, and may exhibit a strong temperature dependence of the lifetime. This candidate mechanism may also be relevant to describing molecular transport.
- (6) As partially noted above, carry out further work towards the development of an extended theory which predicts both electrical behavior and the amount of transmembrane transport of molecules. Here the involvement of membrane proteins, particularly channel forming proteins, is believed to be important. Such a theory should include hindered diffusion as a primary mechanism, particularly for long times involving persistent metastable pores. However electrokinetic mechanisms such as electrophoresis and electroosmosis which may also operate during the time the transmembrane potential is non-zero. The general goal is to predict the number of molecules which move across a cell membrane, and also (because of the fundamentally statistical nature of the theory, and the statistical orientation of non-spherical cells) the distribution of transport within a cell population.⁵

Throughout we have sought quantitative estimates which can be compared to the results of experiments by ourselves and others.

SUMMARY

We have completed our initial extension of a transient aqueous pore theory of electroporation. This improved model yields descriptions of four key aspects of complex electrical behavior:

- Reversible electrical breakdown (REB) leading to complete membrane discharge
- Incomplete REB (discharge halts at $U > 0$)
- Rupture (mechanical) with its characteristic slow, sigmoidal electrical discharge
- Membrane charging without dramatic behavior at small U

The extended theory quantitatively describes this complex set of behavior. This improved version eliminates the use of sharp conduction criteria for pores, and instead uses a more realistic continuous conduction in which an estimate of the Born energy is used with a Boltzmann factor to describe the reduced conductivity of a pore in a low (compared to water) dielectric constant membrane. This version also eliminates the use of an assumption concerning the number of pores present in a membrane at equilibrium, and instead utilizes creation and destruction rates for pores. This version further assumes a realistic minimum pore size, based on molecular sizes. Finally, this version provides the first unified and quantitative description of the several dramatic electroporation-related phenomena listed above.

We are now continuing to make progress towards combining the improved version (which describes the very early electrical events) with a model for pore-membrane protein interactions (expected to be relevant to the long-lived high permeability state). Although still fraught with difficulties, we anticipate that this approach will lead to a reasonable description of cell membrane electroporation, wherein first dramatic electrical events occur, followed by two phases of membrane recovery (fast, complete resealing of most pores, and slow, metastable pore-protein complexes which recover, probably through a thermally activated process). Finally, we expect that mass transport through both the fast recovering pores and slowly recovering pores will be significant, with a combination of hindered diffusion and electrokinetic transport being significant for the fast recovering pores, and primarily hindered diffusion being important through the slowly recovering pore-protein complexes. Throughout, we will continue to emphasize theoretical development which can lead to the prediction of experimental results, thereby allowing direct comparisons.

COPY OF SUBMITTED MANUSCRIPT

Because of the complexity and length (47 pages) of the calculations, text and computed graphs which show how one can quantitatively describe the electrical behavior associated with electroporation in an artificial planar bilayer membrane, we have not attempted to summarize the calculation and its results, as this could be misleading. Instead we have provided a complete copy of the manuscript:

Barnett, A. and J. C. Weaver "Electroporation: A Unified, Quantitative Theory of Reversible Electrical Breakdown and Rupture" (submitted).

Figures 5 through 12 provide illustrations of the behavior of the model, and demonstrate that much of the complex behavior observed in experiments is actually described by the model.

References

1. Zimmermann, U., "Electrical Breakdown, Electroporation and Electrofusion," *Rev. Physiol. Biochem. Pharmacol.*, vol. 105, pp. 175 - 256, 1986.
2. Potter, H., "Electroporation in Biology: Methods, Applications, and Instrumentation," *Analyt. Biochem.*, vol. 174, pp. 361 - 373, 1988.
3. Neumann, E., A. Sowers, and C. (Eds) Jordan, *Electroporation and Electrofusion in Cell Biology*, Plenum, New York, 1989.
4. Weaver, J. C. and K. T. Powell, "Theory of Electroporation," in *Electroporation and Electrofusion in Cell Biology*, ed. E. Neumann, A. Sowers and C. Jordan, pp. 111 - 126, Plenum, 1989.
5. Bartoletti, D. C., G. I. Harrison, and J. C. Weaver, *The Number of Molecules Taken Up by Electroporated Cells: Quantitative Determination*. (submitted)



Accession For	
NTIS CRA&I	<input checked="" type="checkbox"/>
DTIC TAB	<input type="checkbox"/>
Unannounced	<input type="checkbox"/>
Justification	
By	
Distribution /	
Availability Codes	
Dist	Avail and Spec
A-1	

(Submitted)

**Electroporation: A Unified, Quantitative
Theory of Reversible Electrical Breakdown and Mechanical Rupture
in Artificial Planar Bilayer Membranes**

**Alan Barnett and James C. Weaver
Harvard-MIT Division of Health Sciences and Technology
Cambridge, MA 02139, U.S.A.**

April 5, 1989

ABSTRACT

We present a quantitative theory of electroporation of artificial lipid bilayer membranes. Assuming that aqueous pores cause electroporation, we describe the pore population of the membrane by the density function $n(r, t)$, where $n(r, t) dr$ is the number of pores with radius between r and $r + dr$ at time t . To write a set of differential equations for the evolution of $n(r, t)$, we assume that there is a minimum pore size r_{\min} , that pores of radius r_{\min} are created and destroyed by thermal fluctuations, and that the pore creation rate is proportional to $\exp(-\frac{U^2}{kT})$, where U is the membrane voltage, we derive a relation between pore size and pore conductance, we use the expression for the pore energy previously derived by Pastushenko and Chizmadzhev, and we include a model of the external circuit equation numerically. We solve the equations numerically and compare the solutions to the results of charge pulse experiments.

In a charge-pulse experiment a membrane suffers one of four possible fates: (1) a slight increase in electrical conductance, (2) mechanical rupture, (3) partial reversible electrical breakdown, resulting in incomplete discharge of the membrane, or (4) reversible electrical breakdown (REB), resulting in complete discharge of the membrane. In agreement with experiment, our theory describes these four fates and predicts that the fate in any particular experiment is determined by the properties of the membrane and the duration and amplitude of the charging pulse.

INTRODUCTION AND BACKGROUND

Electroporation is a set of related phenomena, caused by the formation of aqueous pores, that are observed in both natural and artificial bilayer membranes in response to a large applied electric field. In planar artificial membranes these phenomena include reversible electrical breakdown (REB) and membrane rupture¹, while in cells REB is followed by a transient high permeability state.²⁻⁵ Much of the recent interest in electroporation relates not to electrical behavior, but rather to the significant fluxes of molecules across cell membranes that occur during the high permeability state.⁶ Most applications of

electroporation have involved the introduction of genetic material into cells, but the large transient molecular fluxes have much wider applications. Although such molecular transport itself has sometimes been termed "electroporation"⁷, the transient molecular flux is only one consequence of electrically generated large pores; we therefore use the term "electroporation" to refer to all pore phenomena associated with a large transmembrane potential difference.

Although the topology of cells differs from that of planar membranes, many features of REB in planar membranes and in cell membranes are the same.⁸ The planar geometry, which permits easy access to both sides of the membrane, and the simplicity of bilayer membranes that lack proteins combine to make artificial membranes a good model system. The insight gained from the study of artificial membranes will be a good foundation on which to build a theory of electroporation in biological membranes. The remainder of this paper deals exclusively with artificial bilayer membranes.

First we discuss two types of experiments used for studying electroporation of artificial planar bilayer membranes, then we describe phenomena observed in the experiments, and finally we derive and discuss a theory that can explain many observations by providing a complete description of the observable electrical behavior of artificial bilayer membranes, including the trans-membrane potential $U(t)$ and the membrane conductance $G(t)$.

ELECTROPORATION EXPERIMENTS: VOLTAGE CLAMP AND CHARGE PULSE

There are two major types of electroporation experiments: voltage clamp and charge pulse. Both types of experiment use apparatus similar to that shown in Figure 1. The apparatus consists of a vessel filled with an electrolytic solution.^{1,8-12} A planar lipid bilayer membrane spans the vessel, dividing it into two compartments. In each compartment is a planar electrode oriented parallel to the membrane. When the electrodes are at different potentials, the electric field is perpendicular to the membrane. An external circuit applies a signal to the electrodes and measures the response of the system.

An equivalent circuit for a voltage clamp experiment is shown in Figure 2 and for a charge pulse experiment is shown in Figure 3. We model the membrane as a capacitor C in parallel with a resistor $\frac{1}{G(t)}$. The membrane is in series with the resistor R_E which represents the electrolyte and the electrodes (we neglect the capacitance of the electrodes, which is small). The external circuit consists of a voltage source with internal resistance R_T in series with an ammeter for a voltage clamp experiment and of a current source with internal resistance R_N in parallel with a voltmeter for a charge pulse experiment.

In a voltage clamp experiment, a voltage waveform $U_i(t)$, typically a series of step functions, is applied to the electrodes and the current I_m , the sum of the charging current to the "membrane capacitor" and the leakage current through the "membrane resistor" is measured. The quantity of interest is the membrane conductance $G(t)$. When the applied voltage is not changing $G(t)$ is related to $U_i(t)$ and to the measured current $I_m(t)$ by the equation

$$G(t) = \frac{U_i(t) - I_m(R_E + R_T)}{I_m + (R_E + R_T)C \frac{dI_m}{dt}} \quad (1)$$

Typically, the amplitude of the applied voltage is of the order of 0.2 v - 0.7 v, and the duration of the pulse is of the order of milliseconds or longer.⁸

In a charge pulse experiment a current waveform $I_i(t)$, typically a square wave, is applied to the electrodes and at the end of the pulse the switch is opened.¹ After the pulse, the membrane conductance $G(t)$ is related to the measured voltage U_m by the equation

$$G(t) = -C \frac{d(\ln U_m)}{dt} \quad (2)$$

Since a membrane undergoing REB can discharge in less than a microsecond, the time scale of charge pulse experiments is much shorter than the time scale of voltage clamp experiments. Although the theory we develop is applicable to the behavior of membranes on all time scales of interest, in this paper we confine ourselves to the discussion of charge pulse experiments and short time scales.

MEMBRANE FATES IN CHARGE PULSE EXPERIMENTS

Benz *et al*¹ have observed that a membrane in a charge pulse (pulse length = 0.4 μ s) experiment suffers one of four possible fates:

- (1) Slight increase in conductivity
- (2) Irreversible rupture
- (3) Incomplete reversible electrical breakdown, or
- (4) Reversible electrical breakdown.

In case 4, the membrane conductance increases by up to eight orders of magnitude, causing the membrane to discharge completely in less than 1 μ s. The membrane then recovers slowly to its original state. In case 3, the membrane conductance increases by several orders of magnitude; the membrane then begins to discharge with a characteristic time of about 1 μ s, but the membrane recovers before the membrane discharges completely. In case 2, the membrane conductance increases sharply after a delay of many microseconds and never recovers its original properties following discharge. In case 1, the membrane conductance increases slightly during the pulse and slowly returns to its original value. The fate of the membrane in any given experiment is determined by the properties of the membrane and the duration and magnitude of the applied pulse. A successful electroporation theory must predict the outcome of any given experiment and explain the differences between the four fates in terms of a reasonable physical model.

In the present theory we hypothesize that a membrane contains a population of aqueous conducting pores that are created and destroyed by thermal fluctuations. Our "standard membrane" in equilibrium at room temperature and with membrane voltage $U = 0$ contains about seven pores. We will show that our theory gives the following explanation for the four fates:

If a small amplitude pulse is applied to the membrane experiment, the membrane charges with a characteristic RC time constant. The membrane resistance does not increase significantly, as the pore

creation rate will not change much from its value for $U = 0$. If the pulse amplitude and duration are large enough to cause rupture, the electric field across the membrane increases the pore creation rate and causes the resulting pores to increase in size. The membrane conductance increases, but not enough to cause the membrane to discharge rapidly. Eventually, one or more pores become large enough to become unstable. As the large pore grows, the membrane conductance increases and the membrane discharges, but the unstable pore continues to grow until the membrane ruptures. If the pulse amplitude and duration are large enough to cause REB, the enhancement of the membrane conductance is sufficient to discharge the membrane before any pores become unstable; the pores then shrink in size and their number decreases, and the membrane returns to its initial state undamaged. For partial REB, the discharge is incomplete; the membrane conductance increases sufficiently rapidly that the membrane remains charged to .1 v or so.

MATHEMATICAL FORMULATION

We now present a derivation of our theory, which is an extension and improvement of previous work.¹³⁻¹⁵ Consider a membrane in an electroporation experiment, such as shown in Figure 1. Let $n(r, t) dr$ be number of pores in the membrane with radius between r and $r + dr$ at time t . The density function $n(r, t)$ obeys Smoluchowski's equation¹⁶

$$\frac{\partial n}{\partial t} = D_p \left[\frac{\partial^2 n}{\partial r^2} + \frac{\partial}{\partial r} \left[\frac{n}{kT} \frac{\partial \Delta E}{\partial r} \right] \right] \quad (3)$$

where D_p , the diffusion constant for the pore radius, is independent of r ¹⁷, k is Boltzmann's constant, T is the absolute temperature, and ΔE is the pore "energy", a function of r and U with dimensions of energy that has the property that $-\left(\frac{\partial \Delta E}{\partial r}\right)_U$ is the effective force acting to increase the pore size.

Equation (3) is valid for $r_{\min} \leq r \leq r_{\max}$. We discuss the question of the appropriate values of r_{\min} and r_{\max} in the section on boundary conditions.

Equation (3) can be derived from the assumption that j , the flux density of pores in radius space, is given by

$$j = -D_p \left[\frac{\partial n}{\partial r} + \frac{n}{kT} \frac{\partial \Delta E}{\partial r} \right] \quad (4)$$

The first term in the right member of Equation (4) is the "diffusion flux density" due to random changes in the size of the pores due to thermal fluctuations. The second term is the "drift flux density" due to the action of the radial force acting to change the pore size. If pores are neither created nor destroyed (except at the "boundaries" r_{\min} and r_{\max}), j obeys the continuity equation

$$\frac{dn}{dt} + \frac{dj}{dr} = 0 \quad (5)$$

Use of Equation (4) to eliminate j in Equation (3) yields Equation (1).

To use Equation (3) to describe a membrane we must specify the functional dependence of ΔE on U and r , apply appropriate initial and boundary conditions, and write an additional equation which relates $U(t)$ to $n(r,t)$. First we discuss the function ΔE .

THE PORE "ENERGY" ΔE

The dynamics of the pore population is controlled by the physical forces that act to change pore radius. These forces are of two types: (I) forces due to thermal fluctuations that change rapidly and randomly in time, and (II) forces that are functions of the local electric field and the mechanical configuration of the pore. A complete formulation of the problem would require knowledge of the stress in the membrane for any given configuration. For a given membrane and pore shape, one would solve Maxwell's equations for the electric field, and use the Maxwell stress tensor to compute the forces of electrical origin. The equilibrium shape of the membrane and pore could then be calculated by balancing the mechanical and electrical stresses. One would then have to repeat the calculation.

taking into account thermal fluctuations of the pressure in the bathing solution, the stress in the membrane, and the electric field. This approach is prohibitively difficult. To make the problem tractable, we follow Abidor *et al*¹⁸ and assume that each pore is cylindrical, and is therefore completely described by one parameter, its radius.

We write ΔE as the sum of the mechanical contribution ΔE_M , the electrical contribution ΔE_E , and an arbitrary constant ΔE_0 .

$$\Delta E = \Delta E_M + \Delta E_E + \Delta E_0 \quad (6)$$

A simple and physically reasonable form for ΔE_M is^{19, 20}

$$\Delta E_M = 2\pi\gamma r - \pi\Gamma r^2 \quad (7)$$

where Γ is the surface tension of the membrane-water interface, and γ is the edge energy of the pore.

To compute the electrical contribution to the force, we must solve the electrostatics problem.

This is a difficult task, and no adequate formulation of the problem has yet appeared in the literature.

The primary difficulty involves computing the relation between the current density and the electric field in the aqueous phase near the membrane and inside the pores. We follow Pastushenko and Chizmadzhev²¹ and assume that the system can be described by Ohm's law, and that the electrical conductivity σ is constant in each of three different regions:

$$\sigma = \begin{cases} \sigma_e & \text{in the bulk electrolyte} \\ \sigma_p & \text{inside a pore} \\ 0 & \text{inside the lipid} \end{cases} \quad (8)$$

The conductivity σ_e is related to the concentrations C_i and mobilities η_i of the ions in solution by the formula

$$\sigma_e = \sum_i (z_i e)^2 \eta_i C_i \quad (9)$$

where $e = 1.6 \times 10^{-19}$ coulomb, z_i is the charge of the i -th type of ion, and the sum is over all of the different types of ions in the solution. The conductivity inside the pore is given by

$$\sigma_p = \sum_i (z_i e)^2 \eta_i C_i H_i \exp \left[\frac{\mu_i^0}{kT} \right] \quad (10)$$

where H_i , the steric hindrance factor, is a function of the pore radius and of the radius r_i of ion of type i , and μ_i^0 is the standard chemical potential of an ion of type i inside the pore. We use the polynomial approximation for H_i given by Renkin.²²

$$H(r) = \left[1 - \left(\frac{r_i}{r} \right)^2 \right] \left[1 - 2.1 \left(\frac{r_i}{r} \right) + 2.09 \left(\frac{r_i}{r} \right)^3 - 0.95 \left(\frac{r_i}{r} \right)^5 \right] \quad (11)$$

We approximate the standard chemical potential an ion in the pore by the Born energy of a point charge on the axis of an infinite cylinder²¹

$$\mu_i^0 = \frac{(z_i e)^2}{4\pi\epsilon_l r} P \left(\frac{\epsilon_l}{\epsilon_w} \right) \quad (12)$$

where ϵ_l and ϵ_w are the dielectric constants of the lipid and the water, respectively, and the function P has a maximum value of 0.25.²³

To find an approximate solution to the electrostatics problem, we start with the assumptions that the pores are sufficiently far apart that their mutual interaction is negligible, and that the electric field E_p inside a pore is uniform and perpendicular to the plane of the membrane. The electrical force acting to enlarge the pore can be expressed in terms of E_p . The electric pressure difference Δp_{elec} at the pore edge is

$$\Delta p_{elec} = \frac{\epsilon_w E_p^2}{2} - \frac{\epsilon_l E_p^2}{2} \quad (13)$$

where the first term is the electrical pressure in the pore and the second is the electrical pressure in the

adjacent lipid. The electrical contribution to the pore "energy" ΔE_E is -1 times the work done to expand the pore from r_{\min} to r :

$$\Delta E_E = - \int \Delta p_{elec} (2\pi r' h dr') = -\pi h (\epsilon_w - \epsilon_f) \int_{r_{\min}}^r E^2 r' dr' \quad (14)$$

where we have used Equation (13). To use Equation (14), one needs to find an expression for E_p in terms of U . Since the membrane surface is not an equipotential when conducting pores are present, we define U to be the potential difference across the membrane far from a pore. The voltage U can be written as the sum of two terms

$$U = U_p + U_s \quad (15)$$

where U_p is the voltage drop across the pore itself and U_s is the voltage drop in the bulk electrolyte near the ends of the pore. The electric field E_p is related to U_p by

$$E_p = \frac{U_p}{h} \quad (16)$$

where h is the thickness of the membrane. The voltage drops U_p and U_s are related to I_p , the current through the pore, by

$$U_p = R_p I_p \quad (17)$$

and

$$U_s = R_s I_p \quad (18)$$

where the pore resistance R_p and the spreading resistance R_s ²⁴ are

$$R_p = \frac{h}{\pi r^2 \sigma_p} \quad (19)$$

$$R_s = \frac{1}{2\sigma_e r} \quad (20)$$

Because R_s and R_p act as a voltage divider, the equation relating E_p to U is

$$E_p = \frac{U}{h} \frac{R_p}{R_s + R_p} \quad (21)$$

Using Equation (21), we can now rewrite Equation (14) as

$$\Delta E_E = -\frac{\pi(\epsilon_w - \epsilon_l) U^2}{h^2} \int_{r_{\min}}^r \alpha^2 r dr \quad (22)$$

where

$$\alpha(r) = \left[1 + \frac{\pi r \sigma_p(r)}{2h \sigma_e} \right]^{-1} \quad (23)$$

a result first obtained by Pastushenko and Chizmadzhev.²¹ Note that for small values of r , $\alpha \approx 1$,

while for large r both α and the electrical force tend to 0 as $\frac{1}{r}$.

It is convenient to define the constant ΔE_0 such that

$$\Delta E(r_{\min}) \equiv 0 \quad (24)$$

The function $\Delta E(r, U)$ is completely defined by Equations (6) - (12) and (19) - (24). Figure 4 is a plot of ΔE versus r for various values of U . The values of the parameters γ , Γ , ϵ_l , ϵ_w , h , r_{\min} and r_i used in the computation for Figure 4 are given in Table 1.

BOUNDARY AND INITIAL CONDITIONS

Since Equation (3) is a parabolic partial differential equation, appropriate boundary conditions consist of two equations of the form

$$g \left(n, \frac{\partial n}{\partial r} \right) = 0 \quad (25)$$

one valid at $r = r_{\min}$ and the other valid at $r = r_{\max}$ for all times, and an initial condition specifying $n(r)$ for all r within $r_{\min} < r < r_{\max}$ at $t = 0$. The boundary condition

$$j = 0 \quad (26)$$

with j defined by Equation (4), corresponds to the case of a perfectly reflecting "wall" in r space, while the condition

$$n = 0 \quad (27)$$

corresponds to a perfectly absorbing wall. We assume that no pores can exist for $r < r_{\min}$, where r_{\min} is a parameter of the model. Packing constraints require r_{\min} to be somewhat larger than the size of the hydrophilic headgroups (≈ 0.7 nm) that make up the surface of the pore, since the pore wall must consist of at least several phospholipid molecules²⁵. For our calculations we use $r_{\min} = 1.0$ nm.

The problem of pore creation and destruction is unsolved. Theories based on treatment of instabilities in planar membranes can identify conditions for instability onset²⁶⁻²⁸, but do not show that such an instability actually results in pore structures. The formation of depressions or dimples²⁹ and membrane breathing modes³⁰, which might precede pore structure formation, has been considered. None of this work is sufficiently advanced to permit one to compute pore birth or death rates. We are therefore forced to make ad hoc assumptions regarding the birth and death rate. We assume that the number of pores changes due to the creation and destruction of pores of radius r_{\min} , with the consequence that the boundary condition at $r = r_{\min}$ is

$$j = \dot{N}_c - \dot{N}_d \quad \text{at } r = r_{\min} \quad (28)$$

where \dot{N}_c and \dot{N}_d are the creation and destruction rates of pores of radius r_{\min} .

To form a pore, which can be thought of as an excitation of the membrane, the membrane must go through configurations which are energetically unfavorable. We characterize this transition by introducing a potential barrier Λ . We expect that this potential barrier will be a function of U . Because the electrical energy is proportional to U^2 (for $r = r_c$, $U = U_p$) we further assume that

$$\Lambda = \delta_c - a U^2 \quad (29)$$

where δ_c and a are constants. Introducing an Arrhenius factor, we write

$$\dot{N}_c = v \exp \left[-\frac{\delta_c - aU^2}{kT} \right] \quad (30)$$

where the attempt rate v is a constant with dimensions of inverse time. This expression is valid as long as the fraction of the membrane area occupied by pores is small. Assuming that the probability that a pore of radius r_{\min} is destroyed is independent of U_p , we write

$$\dot{N}_d = \chi n(r_{\min}) \exp \left[-\frac{\delta_d}{kT} \right] \quad (31)$$

where χ is a constant with dimensions of velocity. Using Equations (4), (29), (30) and (31), the boundary condition at $r = r_{\min}$ becomes

$$D \left[\frac{\partial f}{\partial r} + \frac{f}{kT} \frac{\partial \Delta E}{\partial r} \right] = \chi f(r_{\min}) \exp \left[\frac{\delta_d}{kT} \right] - v \exp \left[-\frac{\delta_c - aU^2}{kT} \right] \quad (32)$$

We now consider the boundary condition at $r = r_{\max}$ and the related issue of large pores. In the follow paragraphs we argue that the large pores, whose unlimited growth causes membrane rupture, form a distinct sub-population that must be treated separately from the small pores, and we derive an equation to describe them. The limiting size separating the large pores from the small pores is r_{\max} , and the boundary condition that we apply at r_{\max} joins together the two sub-populations.

We begin by defining $r_c(U)$ to be the largest value of r for which $\frac{\partial \Delta E}{\partial r} = 0$. For $r > r_c$, ΔE is a monotonically decreasing function of r . This means that a large pore is unstable, and can grow until the membrane ruptures. For r sufficiently large, the "drift flux" term in Equation (4) is much larger than the "diffusion flux" term, and the probability that such a large pore will decrease in size is

very small.

For the description of the small pores, it is therefore appropriate to use any value of r_{\max} that is sufficiently large, and to apply the "absorbing wall" condition (Equation (27)) there. In the numerical simulations, we set $r_{\max} = 2 r_c(0)$. The presence of a pore of radius $2r_c(0)$ ($\approx 2 \times 10^{-6}$ cm) does not mean that the membrane has already ruptured, as such a pore is still very much smaller than the membrane ($\approx .1$ cm); rather, it implies that the membrane is very likely to rupture soon, since the probability of such a pore shrinking again is very small. Until the membrane does rupture, the contribution from the large pore or pores will dominate the membrane conductance G , and therefore determine the time evolution of U .

Because our model is statistical in nature and a single large pore can dominate G , we must consider the effect of fluctuations in the number of large pores. We have defined $n(r) dr$ to be the number of pores with radius between r and $r + dr$. To be more exact, $n(r) dr$ is the average over an ensemble of a large number of identical membranes of the number of pores with radius between r and $r + dr$; the actual number in any particular membrane will in general differ from $n(r) dr$. If the number of pores is large and the conductance of each pore is small, the pore populations of different members of the ensemble are similar and all members are well described by the ensemble average. On the other hand, if the number of pores is small and the conductance of each pore is large, the pore populations of different members of the ensemble are quite different, and no member of the ensemble is well described by the ensemble average.

When one or more large pores dominate G , the growth of the large pores determines the time dependence of G . For this reason it is important to consider the time evolution of the radius of a large pore. We start by observing that Smoluchowski's equation (Equation (3)) is a limiting case of the solution of the problem of a biased random walk³¹. Consider a particle of mass m that obeys the generalized Langevin equation

$$m \frac{d^2 r'}{dt^2} = -\frac{kT}{D_p} \frac{dr'}{dt} - \frac{d\Delta E}{dr'} + g(t) \quad (33)$$

where $g(t)$ is a random function that varies rapidly in time. Proper statistical treatment of Equation (33) leads to the Fokker-Planck equation. Our system corresponds to a "particle" with no inertia, so that statistical treatment leads to the Smoluchowski equation (3). In the limit where m tends to zero and $\left| \frac{d\Delta E}{dr'} \right| \gg |g(t)|$, Equation (33) becomes

$$\frac{dr'}{dt} = -\frac{D_p}{kT} \frac{d\Delta E}{dr'} \quad (34)$$

Thus we see that "velocity" of the "particle" is determined by the balance between the drag and the driving force.

In the interest of clarity, we also give an alternative derivation of Equation (34). In general, r' , the expectation value of the radius of a pore in a membrane described by the density function n , is defined by

$$r' = \frac{\int r n(r,t) dr}{N_p} \quad (35)$$

where N_p is the number of pores in the membrane, i.e.

$$N_p = \int n(r,t) dr \quad (36)$$

We seek an equation for the evolution of r' with time. Consider a membrane with a single pore of radius r_1 ($> r_c(0)$) at $t = 0$. The initial value of the density function is

$$n = \delta(r - r_1) \quad (37)$$

where $\delta(r)$ is the Dirac delta function. Note that $N_p = 1$ at $t = 0$. We assume that, throughout its evolution, both $n(t)$ and $\frac{\partial f}{\partial t}$ are zero at the limits of the range of r . To derive the desired equation,

we take moments of Equation (3). We start by integrating Equation (3) over the entire range of r .

The left member of the resulting equation is $\frac{dN}{dt}$, the time derivative of the number of pores. When

we integrate by parts, we see that the right member is zero. The resulting equation is easily integrated, yielding

$$N_p = 1 \quad (38)$$

Next we multiply Equation (3) by r and integrate over r . The left member of Equation (3) is now just

$\frac{dr'}{dt}$, the time derivative of the expectation value of r . Integrating the right member by parts, the first

term vanishes and the second term becomes

$$\frac{D_p}{kT} \int r \frac{\partial}{\partial r} \left[n \frac{\partial \Delta E}{\partial r} \right] dr = - \frac{D_p}{kT} \int n \frac{\partial \Delta E}{\partial r} dr \quad (39)$$

Since it is the diffusion term that causes $n(r,t)$ to spread, and the diffusion term is small compared to the drift term for $r \gg R_{c(0)}$, we expect n to remain sharply peaked during its subsequent evolution. In this case, the term $\frac{\partial \Delta E}{\partial r}$ can be removed from the integral with the understanding that it is to be evaluated at $r = r'$. The remaining integral is equal to unity, and the resulting equation is clearly equivalent to Equation (34).

We now solve Equation (34). Substitution of Equation (6) for ΔE into Equation (34) and use of Equations (7) - (24) yields an equation that depends upon U , and therefore is coupled to the equation that describes the electrical circuit. But for sufficiently large pores ΔE_E , which contains the U -dependence, is small compared to ΔE_M (compare Equation (7) to Equations (22) and (23)), and can be neglected. The resulting equation is independent of U and can be solved analytically. Setting ΔE equal to ΔE_M and using Equation (7) transforms Equation (34) into

$$\frac{dr'}{dt} = - \frac{2\pi D_p}{kT} (\gamma - \Gamma r') \quad (40)$$

Equation (40) is separable, and its solution is

$$r' = r_c(0) + (r_1 - r_c(0)) \exp\left(-\frac{t}{\tau_d}\right) \quad (41)$$

where the characteristic time τ_d is

$$\tau_d = \frac{kT}{2\pi\Gamma D_p} \quad (42)$$

and r_1 is the initial value of r' .

Note that Equation (41), which describes the evolution of large pores, is deterministic. To combine the statistical description of the small pores with the deterministic description of large pores, we need a criterion for the time of formation of large pores. The probability that a pore becomes large during the interval between t and $t + dt$ is $j(r_{\max}, t) dt$, where j is defined by Equation (4). Since $n = 0$ at $r = r_{\max}$, only the first term in Equation (4) contributes. Since large pores cannot be destroyed (unless the membrane ruptures) and the probability of an additional large pore forming does not depend upon how many large pores already exist, the formation of large pores is a Poisson process. The probability $P(N_l, t)$ that N_l large pores exist at time t is given by the Poisson distribution

$$P(N_l, t) = e^{-\mu} \frac{\mu^{N_l}}{N_l!} \quad (43)$$

where the parameter μ is

$$\mu = \int_0^t j(r_{\max}, t') dt' = -D_p \int_0^t \left[\frac{\partial n(r, t')}{\partial r} \right]_{r=r_{\max}} dt' \quad (44)$$

The probability that the membrane has no large pores at time t is simply

$$P(0, t) = \exp(-\mu) \quad (45)$$

The dominant influence of a small numbers of large pores on the rupture process has an important consequence; thermodynamic fluctuations cause the lifetime of a membrane undergoing rupture to vary from experiment to experiment, even if the experimental setups are identical. This is due to the fact that the creation of the large pore that causes rupture is a random process. The straightforward way to compute t_i , the creation time of the i -th large pore, is to use a random number generator. For the purposes of this paper, it is more convenient to use a completely deterministic model. We therefore require t_i to equal that value of t for which μ equals i ; that is, the first large pore is created at t_1 , when $\mu = 1$, the second at t_2 , when $\mu = 2$, etc, where μ is defined by Equation (44). This is a reasonable scheme, since the Poisson distribution $P(N_i, t)$ (Equation (43)) has the property that μ is the expectation value of N_i , the number of large pores.

Once a large pore forms, its radius as a function of time is given by Equation (41). We therefore define the density function n^* as

$$n^* = n + \sum_i \delta(r - r'(t - t_i)) \quad (46)$$

where n obeys Equation (3) for $r_{\min} < r < r_{\max}$ and equals zero for $r > r_{\max}$, and t_i is the creation time of the i -th large pore.

This division of n into two pieces has one drawback; if the conductance of a single pore of radius r_{\max} is a sizable fraction of the conductance of the membrane, there will be a noticeable discontinuity in $G(t)$ at $t = t_i$. The only way to avoid this discontinuity and still correctly model the effect of the unstable large pores (a pore with radius sufficiently large will always dominate G) is to reformulate the problem and perform a Monte Carlo calculation, which requires much more computing power.

For the initial condition, we assume that at $t = 0$ the membrane is in equilibrium with $U = 0$.

The quasi-steady state solution to Equation (3) can be found analytically; it is

$$n(r) = \begin{cases} \frac{\alpha}{\chi} \exp \left[\frac{\delta_d - \delta_c - 2\pi\gamma(r - r_{\min}) + \pi\Gamma(r^2 - r_{\min}^2)}{kT} \right] & r_{\min} \leq r < r_c(0) \\ 0 & r > r_c(0) \end{cases} \quad (47)$$

THE EXTERNAL CIRCUIT

To close the system of equations, one needs an additional equation to describe the time evolution of U . The membrane is adequately modeled as a capacitor C in parallel with a resistor with conductance $G(t)$. The value of C can be computed with the familiar formula from elementary electrostatics

$$C = \frac{4\pi\epsilon_1 A_m}{h} \quad (48)$$

where A_m is the area of the membrane. The capacitance of the partition that holds the membrane is much smaller than the capacitance of the membrane itself and can be neglected. $G(t)$ can be expressed in terms of an integral over the pore population. The current I_p flowing through a pore of radius r in a membrane with voltage U across it is

$$I_p = \frac{U}{R_s(r) + R_p(r)} \quad (49)$$

where $R_s(r)$ and $R_p(r)$ are defined in Equations (19) and (20), respectively. The current I flowing through the entire membrane is simply the sum of the current flowing through each pore and can be expressed as an integral over $n(r, t)$

$$I = U \int_{r_{\min}}^{\infty} \left[\frac{n(r, t)}{R_s(r) + R_p(r)} \right]^{-1} dr \quad (50)$$

The membrane conductance $G = \frac{I}{U}$ is therefore

$$G(t) = \int_{r_{\min}}^{\infty} \left[\frac{n^*(r,t)}{R_s(r) + R_p(r)} \right]^{-1} dr \quad (51)$$

Figure 3 is a schematic diagram of the entire circuit. A square wave pulse of amplitude I_i is applied to the electrodes for $0 < t < t_{pulse}$, and at $t = t_{pulse}$ the switch is opened. Thus, charge is supplied to the membrane from an external source, but discharge after the switch opens at the end of the pulse can occur only through the membrane. Such a circuit is described by the differential equations

$$C \frac{dU}{dt} = \begin{cases} \frac{I_p R_N}{R_E + R_N} - U \left(G(t) + \frac{1}{R_E + R_N} \right) & \text{if } t < t_{pulse} \\ -\frac{U}{R} & \text{if } t > t_{pulse} \end{cases} \quad (52)$$

and the initial condition

$$U(0) = 0 \quad (53)$$

NUMERICAL SOLUTIONS OF THE EQUATIONS

In the present model, the membrane is characterised by eleven parameters (h , ϵ_i , A , γ , Γ , D , v , χ , δ_c , δ_d , and r_{\min}). Unfortunately, it is difficult to obtain better than an order of magnitude estimate for eight of them from measurements of membrane properties other than electroporation. In principle, one could determine their values by obtaining a "best fit" to experimental data. Because the number of data points one can obtain (the membrane potential $U(t)$ for many values of t for different pulse lengths, applied potentials, solutes, temperatures, etc.) greatly exceeds eight, the system is multiply over determined. Therefore, unless the system is mathematically ill-conditioned, a fitting procedure could be used to determine the values of the parameters. Due to the large amount of computing time required for such a fitting procedure, we do not fit data. Instead, we show that, for one plausible set

of values of the parameters (the "standard membrane"), the present model describes both REB and rupture. In future work we will explore the behavior of the solutions as the parameters are varied.

We solve the Equation (3) using the Crank-Nicholson method. In addition to the eleven parameters that describe the membrane, one must describe the remainder of the experimental apparatus by specifying the temperature T , the electrical conductivity of the solution σ , the radii r_j and charge z_j of each species of small ion, the shunt resistance R_N , the resistance R_E of the electrodes and the solution, and the strength of the current source as a function of time. We use a square wave of amplitude I_0 and duration t_{pulse} for the applied current. We specify the grid size $\Delta r = (r_{max} - r_{min})/m$ and the time step size $\Delta t = \Delta r^2 dt/D_p$ by quoting the values of the parameters m (the number of intervals between grid points) and dt (the time step size in units of the diffusion time based on the grid spacing). The values of all of the parameters used in the numerical calculations are given in Table 1.

RESULTS

Figures 5 - 12 show the results of our numerical calculations. We simulated five charge pulse experiments, which differed only in the amount of injected charge $Q = t_{pulse} I_0$. The pulse length t_{pulse} was $0.4\mu s$ for all five simulations, the amount of injected charge Q was 5 nanocoulombs, 10 nanocoulombs, 15 nanocoulombs, 20 nanocoulombs, and 25 nanocoulombs, and the membrane parameters are given in Table 1. Figures 5 and 6 show $U(t)$, Figures 7 and 8 show $N(t)$, and Figures 9 and 10 show $G(t)$ for all five simulations. The curves in Figures 5 - 10 are labeled by values of the injected charge. There are two time scales of interest: a short time scale (approx $1\mu s$) characteristic of membrane charging and REB, and a long time scale ($\approx 80\mu s$) characteristic of membrane recovery or rupture. Figures 5, 7 and 9 show short time scale behavior, while Figures 6, 8, and 10 show long time scale behavior.

We denote by U_0 the value of the membrane potential at the end of the applied pulse ($t = 0.4\mu s$). Viewed as a function of Q , U_0 increases for small values of Q , reaches a maximum value, and then

decreases again. We denote by $U_{0,c}$ the maximum value of U_0 , and by Q_c the maximum value of Q . For these simulation, $Q_c = 20$ nanocoulombs and $U_{0,c} = 0.94$ v. If the injected charge is greater than Q_c , REB occurs before the end of the pulse, and the membrane conductivity increases so much that the membrane starts to discharge before the pulse ends (see Figs. 5, 7, and 9). A membrane undergoing REB discharges completely in less than 1 μ s. Following discharge the membrane recovers in about 80 μ s. The recovery can best be seen in Figures 8 and 10. The number of pores increases in less than 1 μ s, which looks like a step function in the long time scale plot (Fig. 8), and then decays exponentially back to its equilibrium value. The membrane conductance also increases in about 1 μ s, but it decays in two stages, as can be seen in Figure 10. The first stage, during which the decay is rapid, is caused by the shrinking of the the pores; the second stage, during which the decay is much slower, is caused by the decrease in the number of pores. The membrane returns to its initial state in about 80 μ s. The evolution of G and N during REB are best understood by considering the evolution of $n(r)$ shown in Figure 11. Figure 11 shows $n(r)$ at different times between 0 and 60 μ s for $Q = 20$ nanocoulombs; the curves in Figure 11 are labeled with the time since the begining of the pulse.

Driven by the strong electrical forces, n increases rapidly for all r until REB occurs. As the membrane begins to discharge, the pore creation rate drops, but the force $-\frac{\partial \Delta F}{\partial r}$ still acts to increase the size of existing pores until $t = 0.5 - 0.6$ μ s, by which time the membrane has discharged sufficiently that the electrical force no longer dominates the mechanical force, which favors contraction. The pores shrink faster than they are destroyed, causing a decrease in the average pore size. During this time, N decreases slowly while G decreases rapidly due to the rapid shrinking of the pores. Eventually n relaxes to a quasi-static equilibrium; its shape no longer changes, but its magnitude decreases due to destruction of pores radius r_{min} . During this final phase, G decrease slowly, its variation entirely due to the change in N , as the membrane asymptotically approaches its original state.

For injected charge less than Q_c , REB does not occur during the pulse, and the membrane retains its charge for a much longer time. In this case, the number of pores and the membrane conductance

continue to grow even after the end of the pulse. There even exists a range of Q for which the membrane does not undergo REB until after the end of the pulse. For $Q = 15$ nanocoulombs, the membrane discharges rapidly for t between $0.8 \mu\text{s}$ and $4 \mu\text{s}$, at which time $U = 0.05 \text{ v}$ and the membrane conductance only slightly exceeds the conductance of an unexcited membrane ($\approx 4.5 \times 10^{-9}$). The membrane eventually discharges completely with an RC time constant of about 2 s.

For Q sufficiently small, no breakdown occurs. For $Q = 5$ nanocoulombs, the membrane rapidly charges up to $U \approx 0.25 \text{ v}$. At $t = 80 \mu\text{s}$, the membrane pore population is approaching a quasi-steady state, and the conductance has increased by a factor of about 10. The membrane then starts to discharge with a time constant of about 0.1 s. As the membrane discharges, G decreases and the rate of discharge slows until it approaches the unexcited membrane RC time constant of about 2 s.

Intermediate values of Q lead to the far more interesting case of mechanical rupture. For $Q = 10$ nanocoulombs, the membrane charges up to $U \approx 0.5 \text{ v}$. It remains almost constant for about $5 \mu\text{s}$, during which time the membrane conductance has increased sufficiently to cause the membrane to discharge. As the membrane discharges, G reaches a maximum and begins to decrease at about $t = 15 \mu\text{s}$. Until $t = 30 \mu\text{s}$ the evolution resembles the case $Q = 15$ nanocoulombs, slowed down by a factor of about 5. The resemblance ceases at $t = 31 \mu\text{s}$ at which time G starts to increase again due to the effect of an unstable pore. (The discontinuities in the curve in Figure 10 are artifacts of the technique used to keep track of the large pores; in a real membrane $G(t)$ is continuous.) As G increases the membrane discharges more and more rapidly, until it is completely discharged by $t = 72 \mu\text{s}$. The unstable pore continues to grow until the membrane ruptures. The time constant for the exponential growth of the unstable pore is given by Equation (42). For the present example, $\tau_d = 13 \mu\text{s}$. The evolution of n leading to mechanical rupture is shown in Figure 12.

DISCUSSION

We have presented a quantitative theory of electroporation of lipid bilayer membranes. The theory successfully describes the four different fates of membranes in charge pulse experiments. We have not fit any data, but rather we have performed numerical "experiments" with a "standard membrane". While our results qualitatively agree with the experimental work of Benz *et al*¹, comparison of our results with theirs shows the following differences:

- (1) The membrane voltage at the end of the pulse $U(t_{pulse})$ for our "standard membrane" is a much stronger function of the injected charge than is observed experimentally.
- (2) The time delay before membrane rupture for our "standard membrane" is shorter by a factor of about 5 than is observed experimentally.

We do not know how much the agreement with experiment can be improved by changing the values of the parameters; we plan to explore this question in the future.

If the data cannot be fit better by changing the values of the parameters, there are several areas in which the model can be improved. Improved approximations for ΔE and better modeling of pore creation and destruction might improve agreement with experiment. In addition, the current-voltage relation of a pore is probably not linear^{12,32}, and this might effect the results.

Another topic for future work is modeling voltage clamp experiments, which deal with smaller trans-membrane voltages and longer time scales. Unfortunately, simulation of a voltage clamp experiment with our present computer program takes a prohibitively long time; we would need to reduce the running time by a factor of 1000.

In summary, we believe that the present theory correctly describes the overall features of electroporation, but further work is required to obtain detailed quantitative agreement with experiment.

A_m	membrane area	1.45 mm ²
C	capacitance of membrane	9.61 nF
D	diffusion constant	5×10^{-10} cm ² /s
dt	time step size (in units of $D/(\Delta r)^2$)	0.5
h	membrane thickness	2.8 nm
kT	temperature	4×10^{-14} ergs
R_E	series resistance of electrolyte, electrodes, and wires	30 Ω
R_N	internal resistance of current source	50 Ω
r_{max}	large pore creation size	40 nm
r_{min}	minimum pore radius	1 nm
r_+	radius of positive ions	0.2 nm
r_-	radius of negative ions	0.2 nm
t_{pulse}	source current pulse length	0.4 μ s
Z_+	charge of positive ions (in units of proton charge)	+1
Z_-	charge of negative ions (in units of proton charge)	-1
γ	pore edge energy density	2 μ ergs/cm
Γ	membrane surface tension	1 erg/cm ²
δ_c	pore creation energy barrier	2.04×10^{-12} ergs
δ_d	pore destruction energy barrier	2.04×10^{-12} ergs
Δr	grid spacing	.0195 nm
ϵ_l	dielectric constant of lipid	2.1 ϵ_0
ϵ_w	dielectric constant of water	80 ϵ_0
ν	pore creation rate prefactor	10^{25} s ⁻¹
σ_e	conductivity of bulk solution	.098 Ω^{-1} cm ⁻¹
χ	pore destruction rate prefactor	10^{18} cm/s

List of Symbols (see also Table 1)

a	coefficient of U^2 in Λ
C_i	concentration of i -th ion species
e	proton charge
E	electric field
E_p	electric field inside a pore
$G, G(t)$	membrane conductance
$H_i(r)$	steric hindrance factor for ion of radius r_i in pore of radius r
I_i	applied current
I_m	measured current
I_p	current through a pore
j	flux density of pores in radius space
$n(r, t)$	probability density function of pores (small pores only)
$n^*(r, t)$	probability density function of pores (including large pores)
$N(t)_p$	number of pores in the membrane as a function of time
N_c	pore creation rate
N_d	pore destruction rate
$P\left(\frac{\epsilon_l}{\epsilon_w}\right)$	Parsegian's function for Born energy
r	pore radius
r_i	radius of ion of type i
R_p	pore resistance
R_s	spreading resistance (includes both sides of the membrane)
t	time since start of pulse
$U, U(t)$	transmembrane potential
U_i	applied voltage
U_m	measured voltage
U_0	transmembrane potential at the end of a square pulse
$U_{0,c}$	maximum transmembrane potential at the end of a square pulse
U_p	voltage drop across a conducting pore
U_s	voltage drop in electrolyte near the ends of a conducting pore (both ends)
$\Delta E(r, U_p)$	pore "energy"
Δp_{elec}	difference in electrical pressure at the pore edge
η_i	electrical mobility of the i -th ionic species
Λ	potential barrier for pore formation
μ_i	standard chemical potential of an ion of species i inside a pore
σ	electrical conductivity
σ_p	conductivity of electrolyte within a pore
τ_d	time constant for growth of an unstable pore

ACKNOWLEDGEMENTS

We thank K.T. Powell for many stimulating discussions. This study received essential support from the Office of Naval Research through Contract N00014-87-K-0479.

FIGURE CAPTIONS

FIGURE 1. The experimental apparatus consists of a vessel filled with an electrolytic solution. The vessel is separated into two compartments by a partition. On each side of the partition is a planar electrode connected to a power supply and a measuring circuit. The membrane spans an aperture in the partition.

FIGURE 2. An equivalent circuit for a voltage clamp experiment using the apparatus shown in Figure 1. The voltage source $U_i(t)$ in series with the resistor R_T models the power supply, the resistor R_E models the electrolyte, electrodes and wires, and the capacitor C in parallel with the resistor $\frac{1}{G(t)}$ model the membrane. The ammeter measures the current $I_m(t)$ flowing through the electrodes.

FIGURE 3. An equivalent circuit for a charge pulse experiment using the apparatus shown in Figure 1. The current source $I_i(t)$ in parallel with the resistor R_N models the power supply, the resistor R_E models the electrolyte, electrodes and wires, and the capacitor C in parallel with the resistor $\frac{1}{G(t)}$ model the membrane. The switch is opened at the end of the current pulse. The voltmeter measures the potential difference $U_m(t)$ between the electrodes.

FIGURE 4. Pore "energy" vs. radius for a membrane described by the parameters listed in Table 1. Each curve is labeled by the corresponding membrane voltage, which ranges between 0 and 1 volt. A pore of radius r_{\min} is stable only for U less than about 0.35 v, and the force favors expansion of pores larger than 20 nm for all values of U .

FIGURE 5. Membrane voltage vs time (short time scale). for a simulated charge pulse experiment. Each curve is labeled by the corresponding value of the injected charge Q . The curves for $Q = 25$

nanocoulombs and 20 nanocoulombs show REB while the others do not. The values of the membrane parameters are given in Table 1.

FIGURE 6. Membrane voltage vs time (long time scale) for a simulated charge pulse experiment. Each curve is labeled by the corresponding value of the injected charge Q . The curves for $Q = 25$ nanocoulombs and 20 nanocoulombs are the spikes at $t = 0$. The curve for $Q = 15$ nanocoulombs shows that the membrane suffered REB at $t = 2\mu\text{s}$, but the membrane recovered before it had time to discharge completely. The curve for $Q = 10$ nanocoulombs shows rupture, while the curve for $Q = 5$ nanocoulombs shows that the membrane conductance did not increase enough to discharge the membrane. The values of the membrane parameters are given in Table 1.

FIGURE 7. Number of pores vs time (short time scale) for a simulated charge pulse experiment. Each curve is labeled by the corresponding value of the injected charge Q . For $Q = 25$ nanocoulombs, N increases from about 6 to about 2×10^8 . The values of the membrane parameters are given in Table 1.

FIGURE 8. Number of pores vs time (long time scale) for a simulated charge pulse experiment. Each curve is labeled by the corresponding value of the injected charge Q . For $Q = 25$ nanocoulombs and 20 nanocoulombs, cases for which REB occurs, N increases to about 10^8 in less than $.5\mu\text{s}$ and then decays exponentially with a time constant of $\approx 4.5\mu\text{s}$. For $Q = 15$ nanocoulombs, N increases rapidly to about 10^5 and remains almost constant for about $4\mu\text{s}$ before the exponential decrease. For $Q = 10$ nanocoulombs, N increases to about 2×10^3 in about $5\mu\text{s}$ and remains almost constant for about $30\mu\text{s}$ before the decay phase. The membrane in this case ruptures. For $Q = 5$ nanocoulombs, N increases to about 40 in $80\mu\text{s}$. N will return to its initial value as the membrane discharges with a time constant of about 2 s. The values of the membrane parameters are given in Table 1.

FIGURE 9. Membrane conductance vs time (short time scale) for a simulated charge pulse experiment. Each curve is labeled by the corresponding value of the injected charge Q . For membranes that undergo REB ($Q = 25$ nanocoulombs, 20 nanocoulombs), G increases by 8-9 orders of magnitude in less than $.3 \mu\text{s}$. The values of the membrane parameters are given in Table 1.

FIGURE 10. Membrane conductance vs time (long time scale) for a simulated charge pulse experiment. Each trace is labeled by the corresponding value of the injected charge Q . The curves for $Q = 25$ nanocoulombs and $Q = 20$ nanocoulombs, the two cases of REB, show a rapid rise in conductance, followed by relaxation to the initial state in two stages. The first stage, during which G decays rapidly, lasts about $1.5 \mu\text{s}$ and is due to the shrinking of the pores. The second stage, during which G decays much more slowly and approaches its initial value, lasts about $80 \mu\text{s}$ and is due to the death of the pores. The curve for $Q = 15$ nanocoulombs is similar to the higher voltage curves, except that REB is delayed and occurs after the end of the pulse, causing the first stage to take $7 \mu\text{s}$. The curve for $Q = 10$ nanocoulombs shows membrane rupture; the conductance increases for $t > 30 \mu\text{s}$ due to the instability of a large pore. (The discontinuities in the curve are an artifact of the algorithm used to treat the large pores.) For $Q = 5$ nanocoulombs, the conductance increases to a new equilibrium value appropriate to its non-zero membrane potential. The membrane will discharge with an RC time constant of about 2 s as the membrane conductance returns to its initial value. The values of the membrane parameters are given in Table 1.

FIGURE 11. n vs. r for a pore undergoing REB. The density function n is of fundamental importance in the present theory of electroporation, even though it is impossible to measure it directly. The curves are labeled by the time in μs since the start of the charging pulse and represent $n(r, t)$ for $Q = 20$ nanocoulombs. The population of pores of all sizes grows for the duration of the pulse (which corresponds to the time of REB). As the membrane rapidly discharges following REB, the pore des-

traction rate increase, causing a depletion in the population of small pores. Large pores then shrink as the population relaxes to its initial state. The values of the membrane parameters are given in Table 1.

FIGURE 12. n vs. r for a pore that ruptures. The curves are labeled by the time in μs since the start of the charging pulse and represent $n(r, t)$ for $Q = 10$ nanocoulombs. Note the presence of a flux of pores (n has a negative slope) through the boundary at $r = 40$ nm for $t > 30$ μs . This flux leads to the creation of the large unstable pores that cause rupture. The probability that a large pore had formed was 0.63 at $t = 32$ μs . The values of the membrane parameters are given in Table 1.

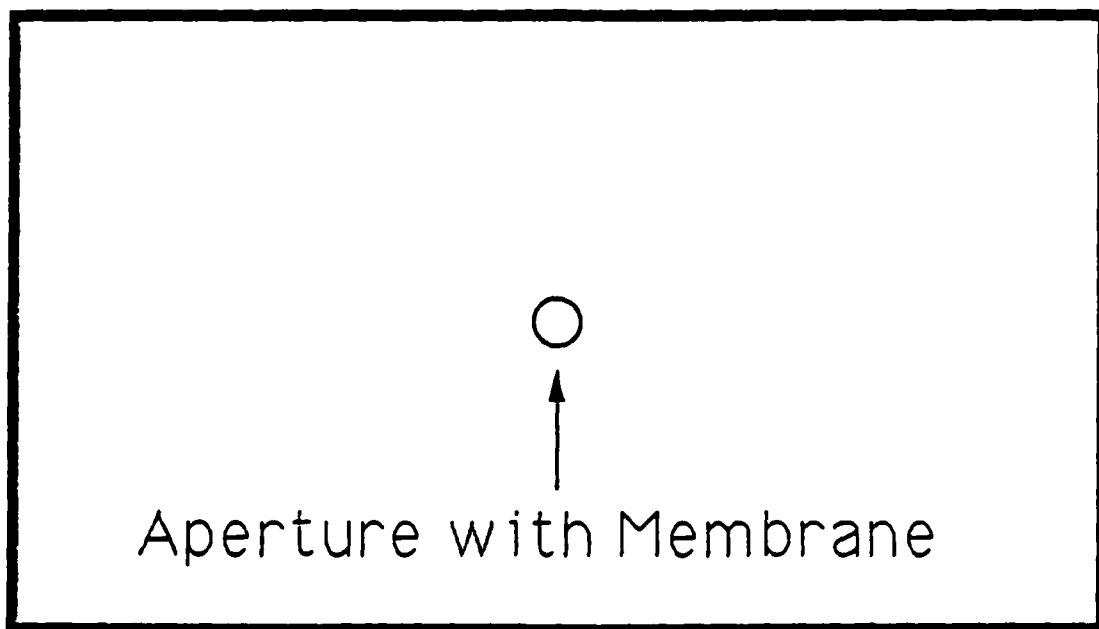
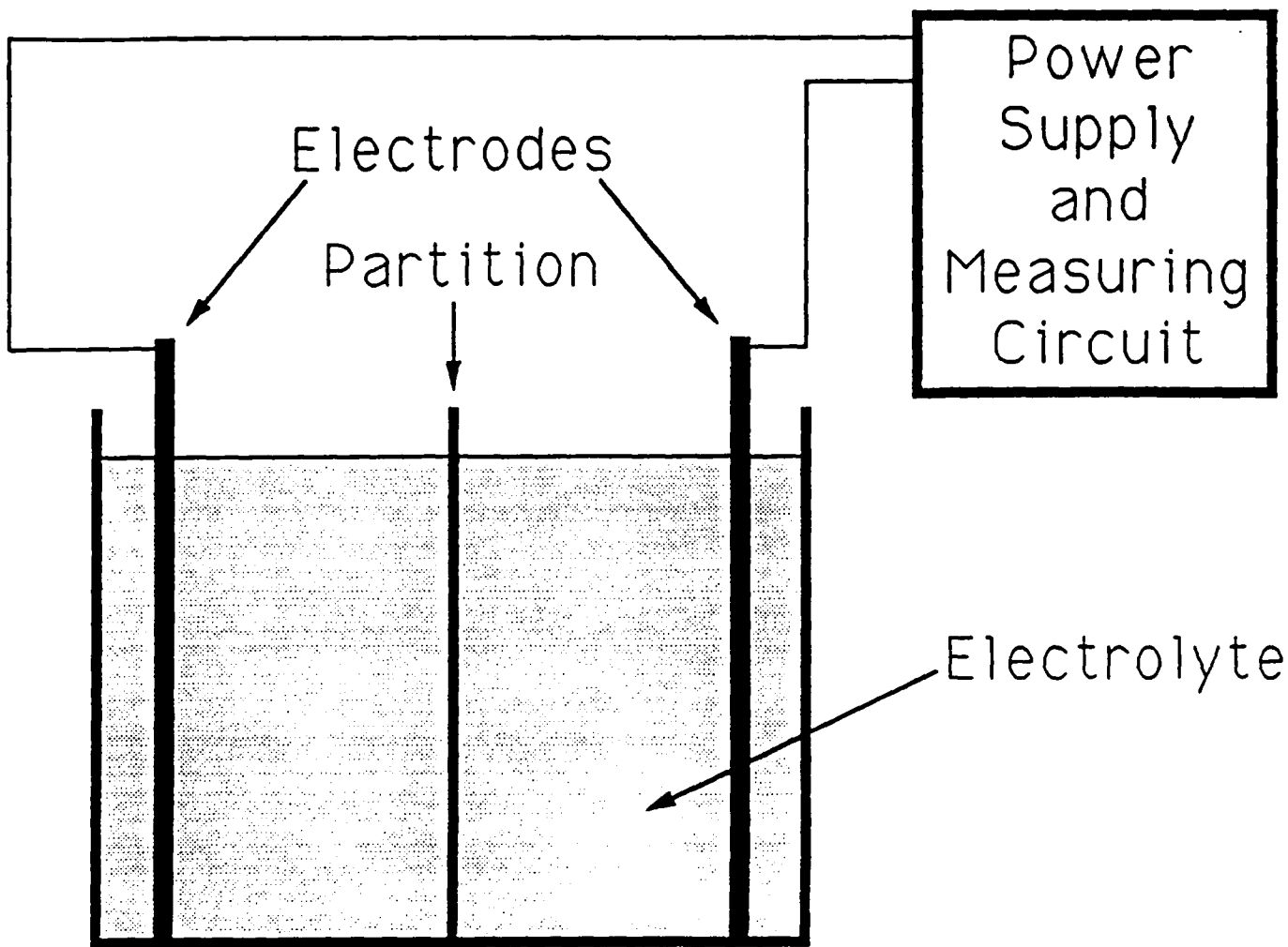
References

1. Benz, R., F. Beckers, and U. Zimmermann, "Reversible Electrical Breakdown of Lipid Bilayer Membranes: A Charge-Pulse Relaxation Study," *J. Membrane Biol.*, vol. 48, pp. 181 - 204, 1979.
2. Neumann, E. and K. Rosenheck, "Permeability Changes Induced by Electric Impulses in Vesicular Membranes," *J. Membrane Biol.*, vol. 10, pp. 279 - 290, 1972.
3. Zimmermann, U., F. Riemann, and G. Pilwat, "Enzyme Loading of Electrically Homogeneous Human Red Blood Cell Ghosts Prepared by Dielectric Breakdown," *Biochim. Biophys. Acta*, vol. 436, pp. 460 - 474, 1976.
4. Kinoshita, K. Jr. and T. Y. Tsong, "Formation and Resealing of Pores of Controlled Sizes in Human Erythrocyte Membrane," *Nature*, vol. 268, pp. 438 - 441, 1977.
5. Sowers, A. E. and M. R. Lieber, "Electropore Diameters, Lifetimes, Numbers, and Locations in Individual Erythrocyte Ghosts," *FEBS Lett.*, vol. 205, pp. 179 - 184, 1986.
6. Neumann, E., A. Sowers, and C. (Eds) Jordan, *Electroporation and Electrofusion in Cell Biology*. Plenum, New York, 1988. (in press)
7. Neumann, E., M. Schaefer-Ridder, Y. Wang, and P. H. Hofschneider, "Gene Transfer into Mouse Lyoma Cells by Electroporation in High Electric Fields," *EMBO J.*, vol. 1, pp. 841 - 845, 1982.
8. Chernomordik, L. V., S. I. Sukharev, S. V. Popov, V. F. Pastushenko, A. V. Sokirko, I. G. Abidor, and Y. A. Chizmadzhev, "The Electrical Breakdown of Cell and Lipid Membranes: The Similarity of Phenomenologies," *Biochim. Biophys. Acta*, vol. 902, pp. 360 - 373, 1987.
9. Benz, R. and U. Zimmermann, "Relaxation Studies on Cell Membranes and Lipid Bilayers in the High Electric Field Range," *Bioelectrochem. and Bioenerg.*, vol. 7, pp. 723 - 739, 1980.

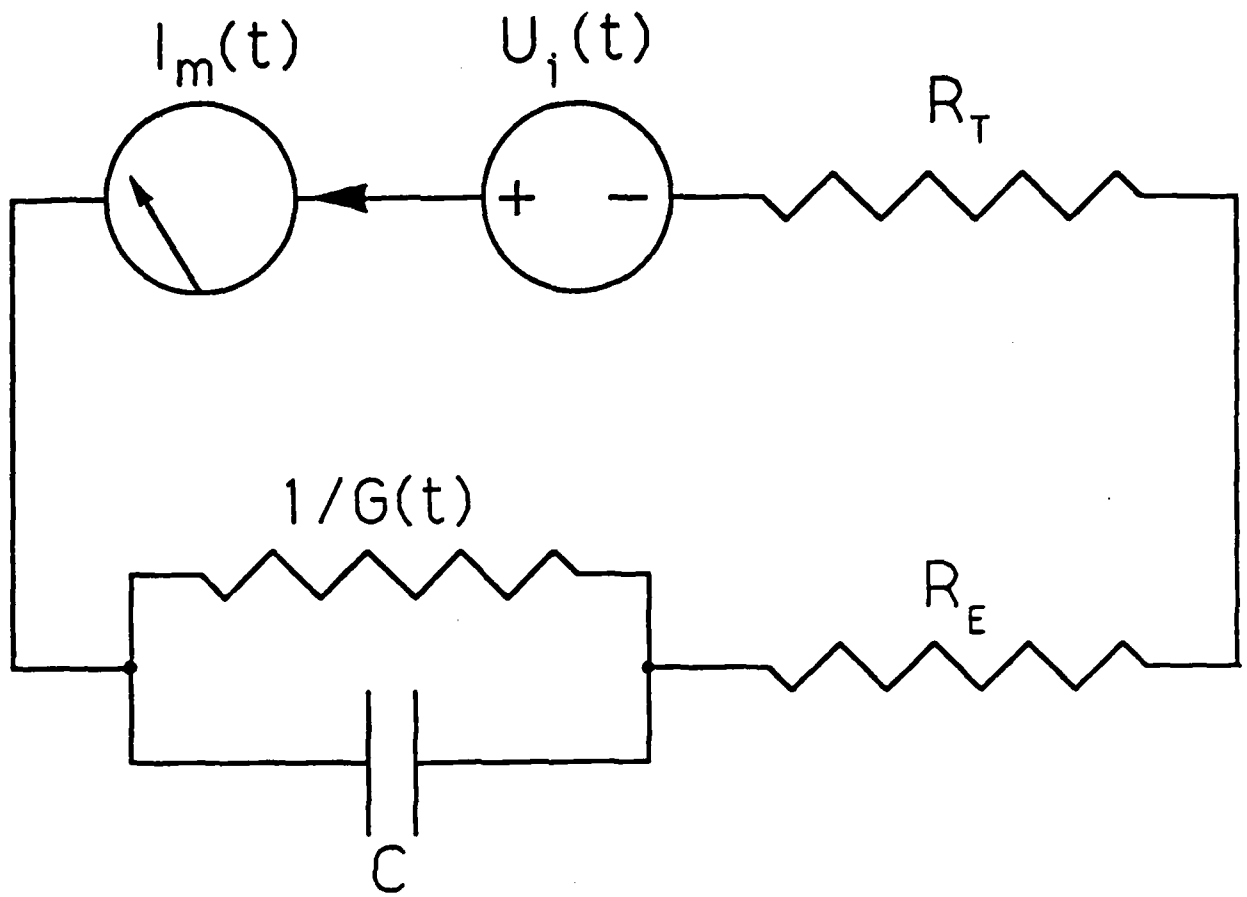
10. Benz, R. and U. Zimmermann, "Pulse-Length Dependence of the Electrical Breakdown in Lipid Bilayer Membranes," *Biochim. Biophys. Acta*, vol. 597, pp. 637 - 642, 1980.
11. Benz, R. and U. Zimmermann, "The Rescaling Process of Lipid Bilayers after Reversible Electrical Breakdown," *Biochim. Biophys. Acta*, vol. 640, pp. 169 - 178, 1981.
12. Glaser, R. W., S. L. Leikin, L. V. Chernomordik, V. F. Pastushenko, and A. I. Sokirko, "Reversible Electrical Breakdown of Lipid Bilayers: Formation and Evolution of Pores," *Biochim. Biophys. Acta*, vol. 940, pp. 275 - 287, 1988.
13. Powell, K. T. and J. C. Weaver, "Transient Aqueous Pores in Bilayer Membranes: A Statistical Theory," *Bioelectrochem. Bioelectroenerg.*, vol. 15, pp. 211 - 227, 1986.
14. Weaver, J. C., R. A. Mintzer, H. Ling, and S. R. Sloan, "Conduction Onset Criteria for Transient Aqueous Pores and Reversible Electrical Breakdown in Bilayer Membranes," *Bioelectrochem. Bioelectroenerg.*, vol. 15, pp. 229 - 241, 1986.
15. Powell, K. T., E. G. Derrick, and J. C. Weaver, "A Quantitative Theory of Reversible Electrical Breakdown," *Bioelectrochem. Bioelectroenerg.*, vol. 15, pp. 243 - 255, 1986.
16. Pastushenko, V. F., Yu. A. Chizmadzhev, and V. B. Arakelyan, "Electric Breakdown of Bilayer Membranes: II. Calculation of the Membrane Lifetime in the Steady-State Diffusion Approximation," *Bioelectrochem. Bioenerget.*, vol. 6, pp. 53 - 62, 1979.
17. Deryagin, B. V. and Yu. V. Gutop, "Theory of the Breakdown (Rupture) of Free Films," *Kolloidn. Zh.*, vol. 24, pp. 370 - 374, 1962.
18. Abidor, I. G., V. B. Arakelyan, L. V. Chernomordik, Yu. A. Chizmadzhev, V. F. Pastushenko, and M. R. Tarasevich, "Electric Breakdown of Bilayer Membranes: I. The Main Experimental Facts and Their Qualitative Discussion," *Bioelectrochem. Bioenerget.*, vol. 6, pp. 37 - 52, 1979.
19. Litster, J. D., "Stability of Lipid Bilayers and Red Blood Cell Membranes," *Phys. Lett.*, vol. 53A, pp. 193 - 194, 1975.

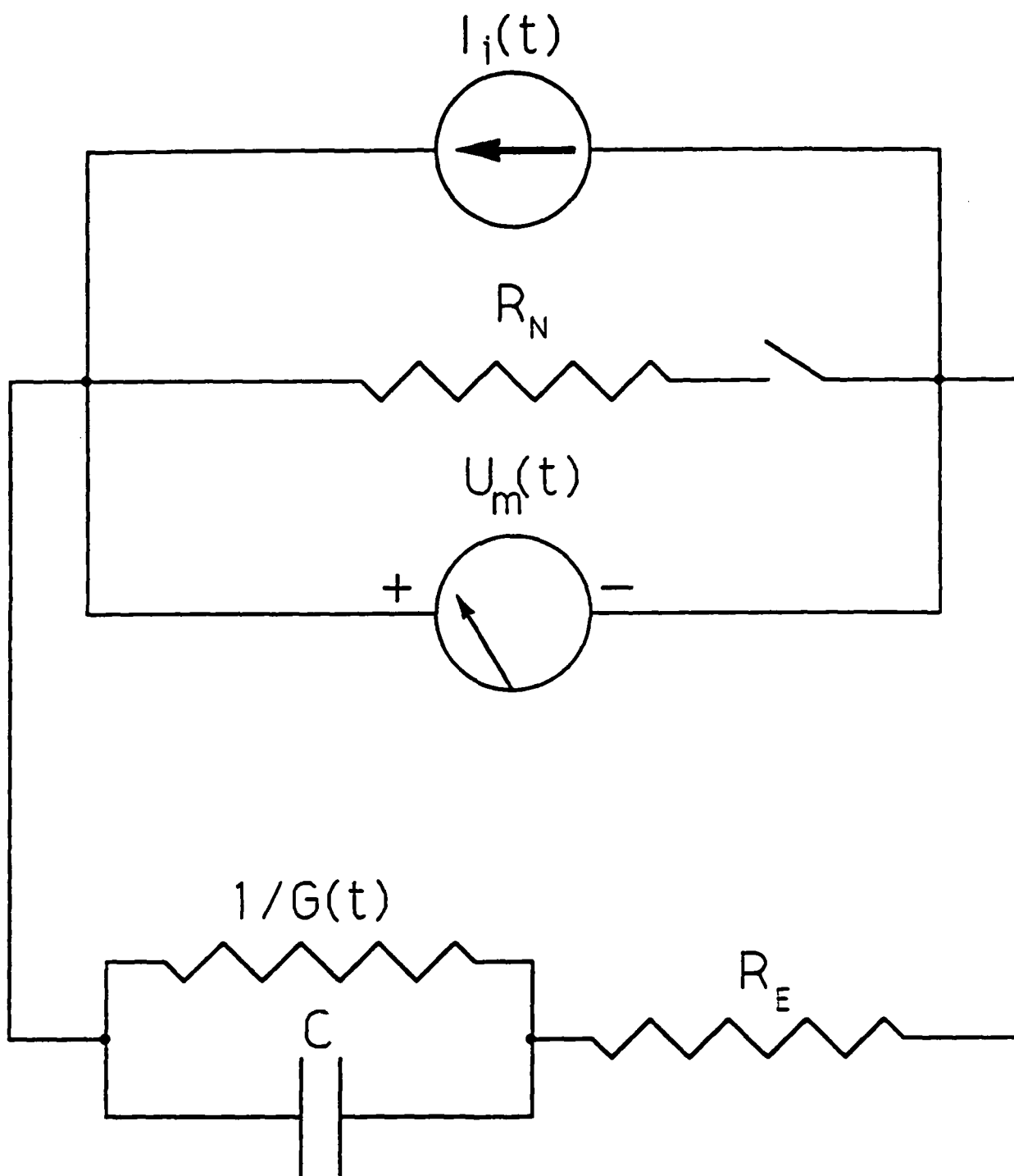
20. Taupin, C., M. Dvolaitzky, and C. Sautrey, "Osmotic Pressure Induced Pores in Phospholipid Vesicles," *Biochemistry*, vol. 14, pp. 4771 - 4775, 1975.
21. Pastushenko, V. F. and Yu. A. Chizmadzhev, "Stabilization of Conducting Pores in BLM by Electric Current," *Gen. Physiol. Biophys.*, vol. 1, pp. 43 - 52, 1982.
22. Renkin, E. M., "Filtration, Diffusion and Molecular Sieving Through Porous Cellulose Membranes," *J. Gen. Physiol.*, vol. 38, pp. 225 - 243 , 1954.
23. Parsegian, V. A., "Energy of an Ion Crossing a Low Dielectric Membrane: Solutions to Four Relevant Electrostatic Problems," *Nature*, vol. 221, pp. 844 - 846, 1969.
24. Newman, J., "Resistance for Flow of Current to a Disk," *J. Electrochem. Soc.*, vol. 113, pp. 501 - 502, 1966.
25. Sugar, I. P. and E. Neumann, "Stochastic Model for Electric Field-Induced Membrane Pores: Electroporation," *Biophys. Chemistry*, vol. 19, pp. 211 - 225, 1984.
26. Crowley, J. M., "Electrical Breakdown of Bimolecular Lipid Membranes as an Electromechanical Instability," *Biophys. J.*, vol. 13, pp. 711 - 724, 1973.
27. Dimitrov, D. S., "Electric Field-Induced Breakdown of Lipid Bilayers and Cell Membranes: A Thin Viscoelastic Film Model," *J. Membrane Biol.*, vol. 78, pp. 53 - 60, 1984.
28. Dimitrov, D. S. and R. K. Jain, "Membrane Stability," *Biochim. Biophys. Acta*, vol. 779, pp. 437 - 468, 1984.
29. Chizmadzhev, Yu. A., V. B. Arakelyan, and V. F. Pastushenko, "Electric Breakdown of Bilayer Membranes: III. Analysis of Possible Mechanisms of Defect Origin," *Bioelectrochem. Bioenerget.*, vol. 6, pp. 63 - 70, 1979.
30. Bach, D. and I. R. Miller, "Glyceryl Monooleate Black Lipid Membranes Obtained from Squalene Solutions," *Biophys. J.*, vol. 29, pp. 183 - 188, 1980.

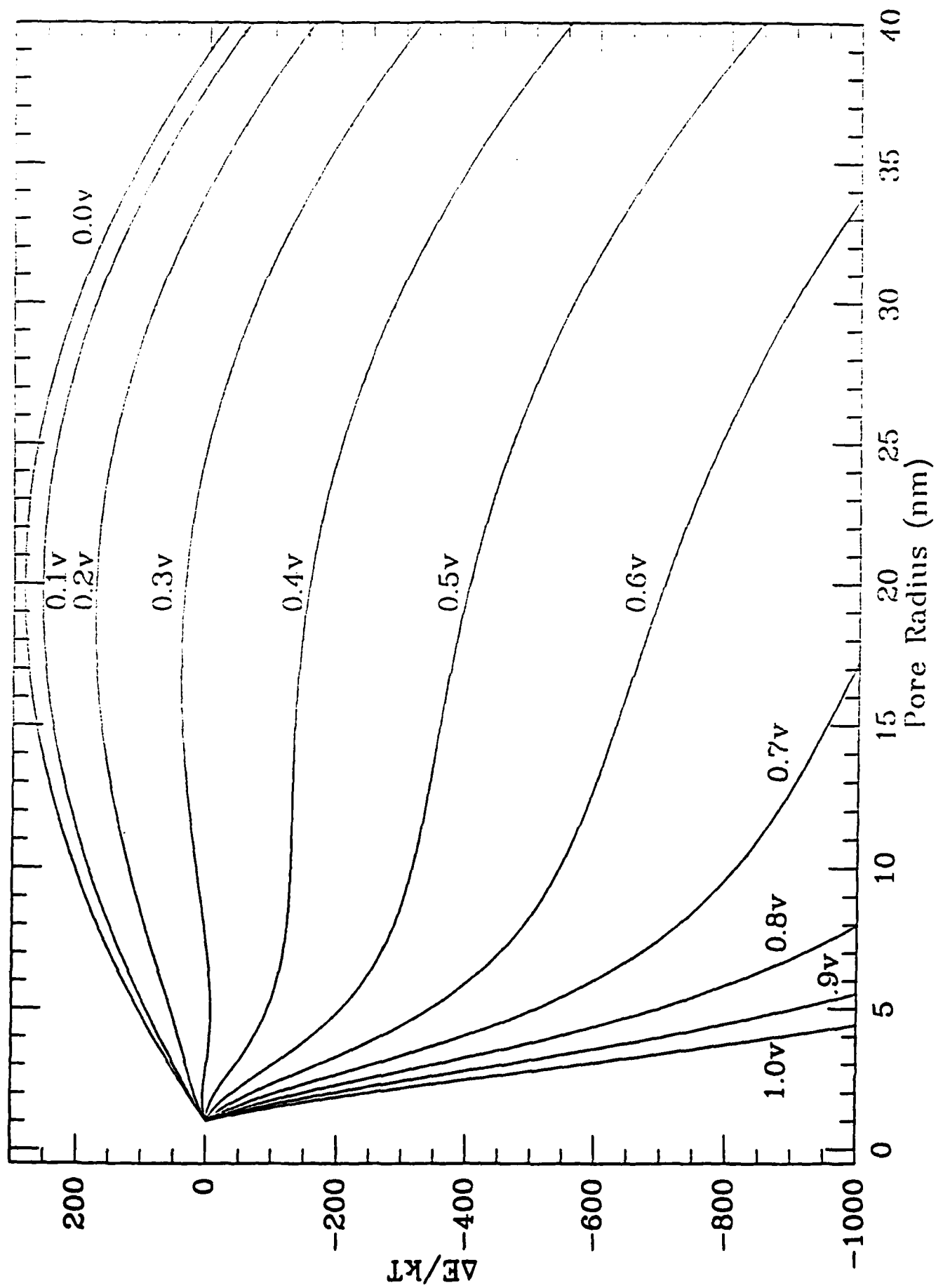
31. Chandrasekhar, S., "Stochastic Problems in Physics and Astronomy," *Rev. Modern Phys.*, vol. 15, pp. 1 - 91, 1943.
32. Barnett, A., "The current-voltage relation of an aqueous pore in a lipid bilayer membrane," *Submitted to Biochimica et Biophysica Acta*, 1989.

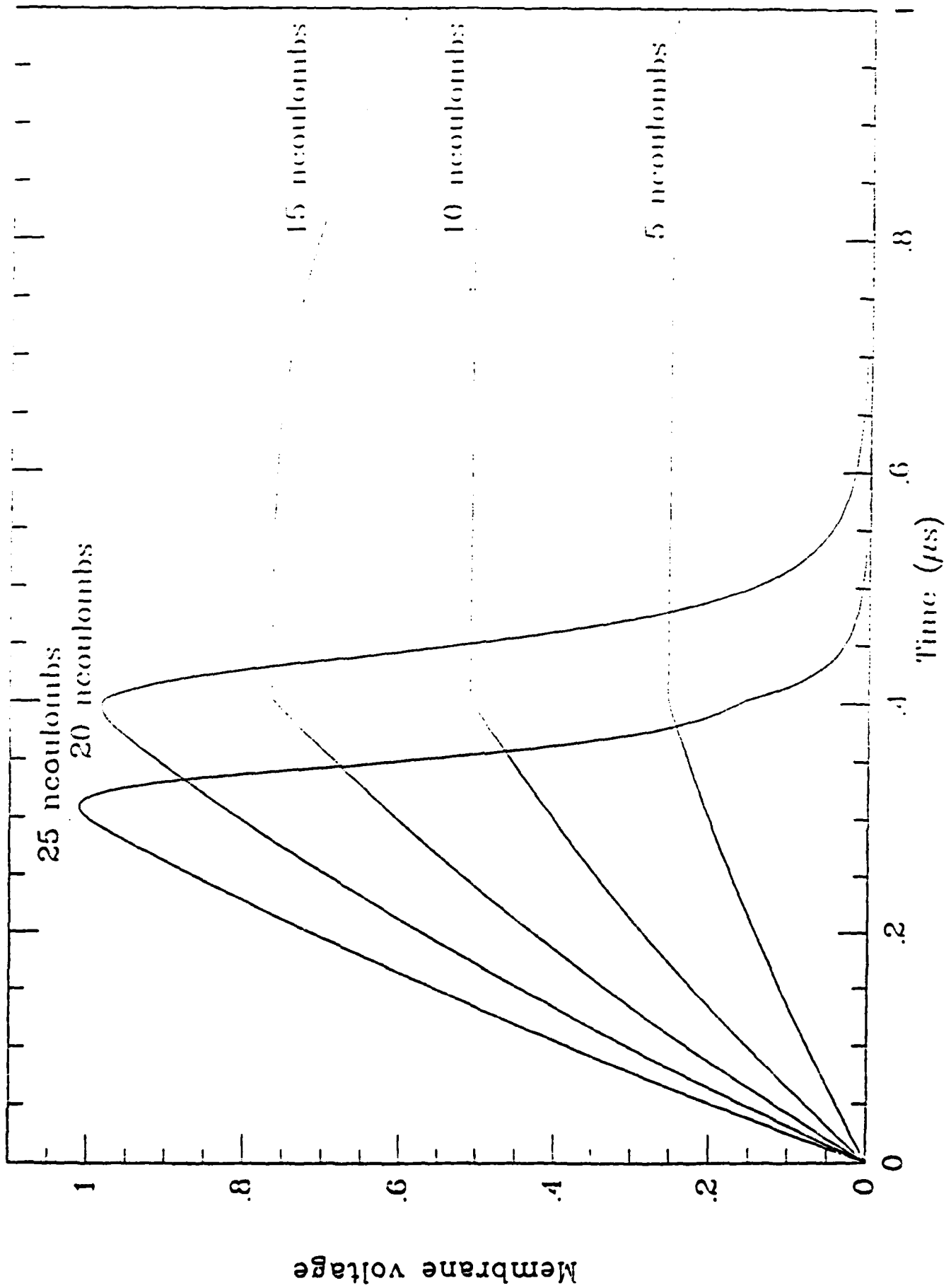


Side View of Partition









Membrane voltage

Time (μ s)

25 nCoulombs
20 nCoulombs

15 nCoulombs

10 nCoulombs

5 nCoulombs

